

Monte Carlo simulation to key parameters of a compensated neutron logger

TUO Xianguo^{1,2} YANG Jianbo^{1,2,*} MU Keliang^{1,2} LI Zhe^{1,2} LONG Qiong²

¹ Provincial Key Lab of Applied Nuclear Techniques in Geosciences, Chengdu University of Technology, Chengdu 610059, China

² Chengdu University of Technology, Chengdu 610059, China

Abstract A compensated neutron logger (CNL) is designed by using Monte-Carlo simulation for lead shield thickness, near-to-far detector spacing range, source-to-detector spacing range, and detector's effective length. The calculated results indicate that the optimum conditions for CNL are 80-mm thick lead plus 1-cm thick LiOH shield in front of the near detector, 250 mm for the near-to-far detector distance (Δr), and the source-to-detector distance (r) of 90mm. Simultaneously, some conclusion also obtained here, near/far detector counting response ratio (R) increases with the effective length of detector, R increases with the porosity for oil and water sandstones, and the oil sandstone is a bit greater than water sandstone.

Key words Monte Carlo, MCNP, Logging, CNL optimal design

1 Introduction

Neutron logging has been used for on-site elemental analysis of the formation and pore fluid, so as to seek clues of minerals, based on neutron-induced nuclear reactions in the well and surroundings^[1]. Compensation neutron logging (CNL) is based on detection of hydrogen, which is the most effective moderator to slow down the neutrons, and which is in much lower content in the skeleton material of a porous formation than that in the water and oil, knowing the hydrogen content enables one to figure out porosity of the formation.

In practical applications, optimal design of CNL is achieved by correct choice of the shield thickness, neutron source distance, near-to-far detector spacing and effective length of the detector, so as to improve the sensitivity of hydrogen index (HI) in identifying oil/gas-bearing layers. But optimization of a system design in an oil field is expensive and time-consuming^[2]. A better way is numerical simulation. In this regard, achievements have been made. The bulk density effect on neutron log response

was studied^[3,4]. In China, Zhang J M, *et al*^[5] did Monte Carlo simulation for the sensitivity of compensated neutron oil logger, and Xia L Z, *et al*^[6] studied structural change effect of the neutron source and detector.

However, more factors shall be simulated, such as the shield thickness, the degrees of interspace, and response ratio of the near/far detectors. Based on our previous research, this work was aimed at optimal design of a CNL system via MCNP programming. After the CNL modeling, optimal parameters of the shield thickness, and positions of the neutron source and the near and far detectors.

2 Modeling

2.1 Theory model

For a point neutron source, the grouping diffusion theory can be applied to an unlimited uniform formation. At a distance of r away from the neutron source, the thermal neutron flux density is^[7]:

$$\Phi_t(r) = L_t^2 (e^{-r/L_t} - e^{-r/L_f}) / [4\pi D_f (L_t^2 - L_f^2) r] \quad (1)$$

Partially supported by National Key Technology R&D Program of China(2008BAK47B04), Innovation Method Work(2008IM040500), National Natural Science Foundation of China(40673058) and Sichuan province Key Technology R&D Program(2008GZ0040, 2008GZ0197)

* Corresponding author. E-mail address: bjiang9@163.com

Received date: 2009-04-27

where $L_t=(D_t/\Sigma_t)^{1/2}$ is thermal neutron diffusion length, $L_f=(D_f/\Sigma_f)^{1/2}$ is slowdown length of fast neutrons, D_f is diffusion coefficient of fast neutron. D_t is diffusion coefficient of thermal neutrons,

Σ_f and Σ_t are macro dispersion sections of fast and thermal neutrons, respectively. Eq.(1) shows that the flux density distribution of thermal neutron is dependent on both the slowdown characteristics of fast neutrons in the formation and the formation absorption condition. Therefore, counting rate of the thermal neutron detector, $N_i(r)$, is proportional to the thermal neutron flux density $\Phi_t(r)^{[5]}$, namely:

$$N_i(r)=K\Phi_t(r) \tag{2}$$

where K is the scale coefficient.

In a CNL, r is the distance between the near detector and neutron source, and Δr is the distance between the near and far detectors, hence the distance of $r+\Delta r$ for the far detector to the neutron source. From Eq. (1) and (2), the near-to-far detector response ratio (R) is

$$R=(r+\Delta r)(e^{\Delta r/L_t-\Delta r/L_f})/r \tag{3}$$

If the formation is of homogeneous mixture of skeleton materials and pores, and the pores are full of fluid containing constant content of hydrogen, the monotonous decline function of the porosity φ can be expressed as $L(\varphi)=1/L_t-1/L_f$. According to Eq.(3), the total differential is^[8]:

$$dR/R=S_\varphi d\varphi+S_\Delta d(\Delta r)+S_r dr \tag{4}$$

where

$$S_\varphi=\partial R/(R\partial\varphi)=-[\Delta r/L^2(\varphi)]dL(\varphi)/d\varphi \tag{5}$$

which represents the relative rate of R caused by the changes of porosity;

$$S_\Delta=\partial R/[R\partial(\Delta r)]=1/L(\varphi)+1/(r+\Delta r)=1/(1/L_t-1/L_f)+1/(r+\Delta r) \tag{6}$$

which represents the relative rate of R caused by the changes of Δr , $\because L_t \ll L_f, \therefore S_\Delta > 0$, and as R increases with Δr , the amplitude is decided by porosity φ ; and

$$S_r=\partial R/(R\partial r)=1/(r+\Delta r)-1/r \tag{7}$$

which represents the relative rate of R caused by r with a fixed Δr , and one finds that $S_r < 0$.

2.2 Simulation model

A ^{252}Cf spontaneous fission neutron source was chosen

for the simulation. The source, with a half-life of 2.64 a, emits neutrons in average energy of 2.3 MeV in a rate of $2.3 \times 10^{12} \text{ s}^{-1} \cdot \text{g}^{-1}$. We used the Watt fissile spectrum model^[9]:

$$p(E)=C \cdot \exp(-E/a) \cdot \sinh(bE)^{1/2} \tag{8}$$

where $E=2.3$ MeV is the neutron energy; $a=0.965$ and $b=2.29$ according to the experimental data of the ^{252}Cf neutron source spectrum, and C is a coefficient. The neutron source was considered as an isotropic source in the simulation using the MCNP code.

As shown in Fig.1, the model for simulation is a well of $\Phi 120 \text{ mm} \times 1200 \text{ mm}$, which is filled with water and has a steel wall ($\rho=7.86 \text{ g/cm}^3$) of 8 mm thick. It is placed eccentrically in a $\Phi 166\text{-mm}$ hole filled with cement ($\text{CaSiO}_3, \rho=1.95 \text{ g/cm}^3$), while the outside is water-sandstone or oil-sandstone of adjustable porosity. The CNL, with a 4-mm thick steel shell ($\rho=7.86 \text{ g/cm}^3$) of 80-mm diameter, is positioned eccentrically in the well. The neutron source is located on the instrument axis. The near and far thermal neutron detectors are ^3He counters with the same external structure but different internal pressures. Each detector differs in sensitive response areas.

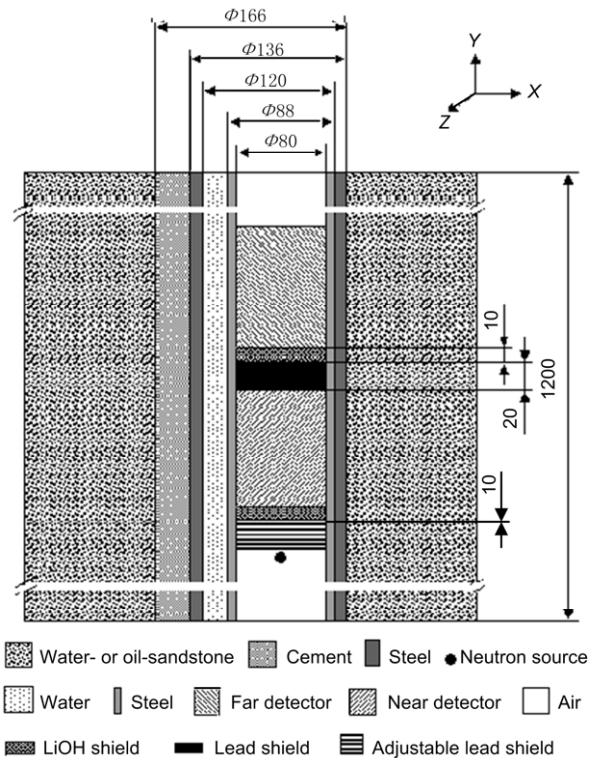


Fig.1 Sketch map of simulation model.

A lead shield of adjustable thickness and a 10-mm thick LiOH shield are placed in front of the near detector; while a 20-mm thick lead shield and a 10-mm thick LiOH shield in front of the far detector. Neutrons from the neutron source penetrate the well, react with the nuclides (especially hydrogen) in the formation, and become super-thermal neutrons or thermal neutrons.

3 Calculation and analysis

The requirements of simulation are: (1) the Watt fissile spectrum; (2) an ENDF/B-VI Rel.1 cross section database; and (3) a computer with Intel Core (TM) 2, CPU for T7200@2.0GHz. The simulation particle number is 2×10^7 and with $<1\%$ of counting errors.

3.1 Shield thickness simulation

In simulation of the shield thickness, porosities the water- or oil-sandstone were 10%, 20%, 30%, 40%, 50% or 60%. Fast neutrons from the neutron source are expected to slow down into thermal neutrons when they are penetrating the formation (X -axis). Because of the shields, the number of fast neutrons in the vertical direction (Y -axis) is the minimum. The adjustable thickness of lead shield is simulated and the relative counting rate (one neutron counts on per unit area) of near/far detector thermal neutron ($E < 0.5$ eV) under different degree of interspaces is recorded. Then the relationship between the lead thickness and near/far detector counting response ratio R (of thermal neutrons) is obtained.

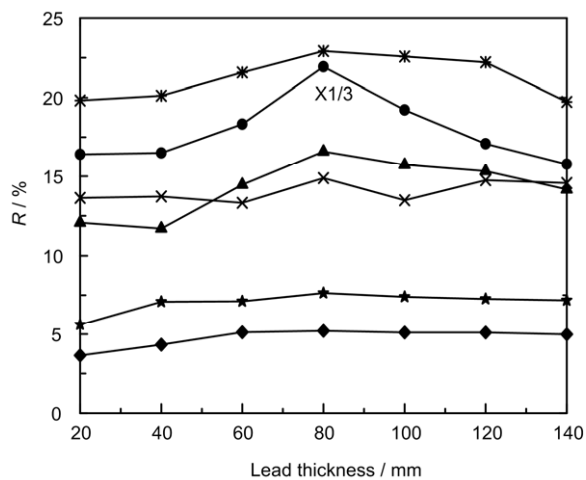


Fig.2 Near-to-far detector response ratio vs. lead thickness at different porosities of the water- and oil-sandstone. Porosities: ◆10%, ★20%, ▲30%, ×40%, ※50%, ●60%

As shown in Fig.2, changes of the R value with the lead thickness are basically in the same trend. With increasing porosity, R becomes larger (the R value is divided by 3 in 60% porosity). In each porosity, R increases with the lead thickness of < 80 mm, where it begins to decrease with increasing lead thickness. Therefore, a suitable lead shield thickness is 80 mm.

3.2 Near-to-far detector distance simulation

The simulation was performed with 80 mm lead shield and 10 mm LiOH shield in front of the near detector, and 20 mm lead shield and 10 mm LiOH shield in front of the far detector. The distance (Δr) between the two detectors changed from 50 mm to 350 mm. The water- and oil-sandstones of 10%, 20%, 30%, 40%, 50% and 60% in porosity were used to simulate the relative change relation of R caused by Δr (Fig.3).

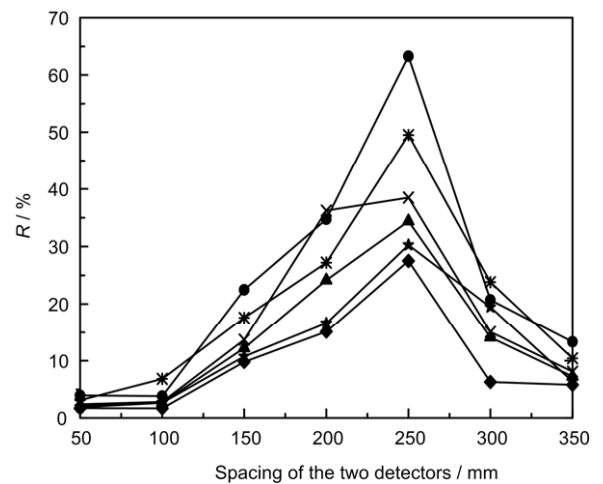


Fig.3 Near-to-far detector response ratio vs. spacing of the two detectors at different porosities of the water- and oil-sandstone. Porosities: ◆10%, ★20%, ▲30%, ×40%, ※50%, ●60%

One sees that the change trend of R is basically the same as the change of Δr in different porosities. The R constantly increases when $\Delta r < 250$ mm, where R starts to decrease dramatically with increasing Δr . Therefore, $\Delta r = 250$ mm is the best choice.

3.3 Source-to-detector distance simulation

This simulation was done with the same experimental conditions as Section 3.2, but the near-to-far detector spacing was fixed at $\Delta r = 250$ mm and the source-to-detector distance (r) varied from 90 mm to 210 mm (Fig.4).

In each porosity, R decreases with increasing r . So, $r=90$ mm, i.e. there is nothing but 80 mm lead and 10 mm LiOH between the neutron source and the detector.

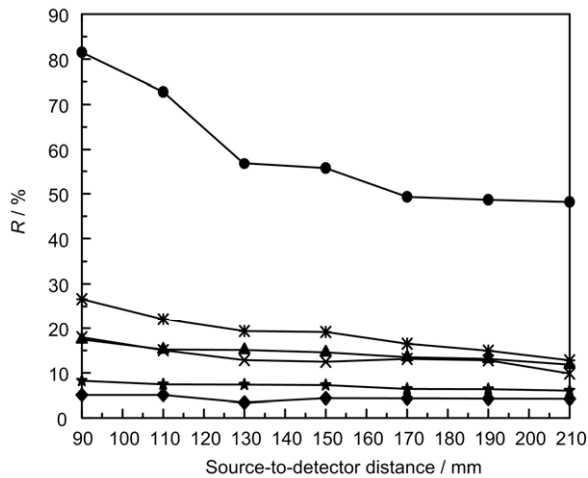


Fig.4 Near-to-far detector response ratio vs source-to-detector distance at different porosities of the water- and oil-sandstone. Porosities: ◆10%, ★20%, ▲30%, ×40%, ※50%, ●60%

3.4 Simulation of the detector effective length

The simulation was performed at $r=90$ mm, with the detector effective length varying from 50 mm to 350 mm, while the other conditions were the same as Section 3.3. The results are shown in Fig.5. The R increases all the way with the detector effective length.

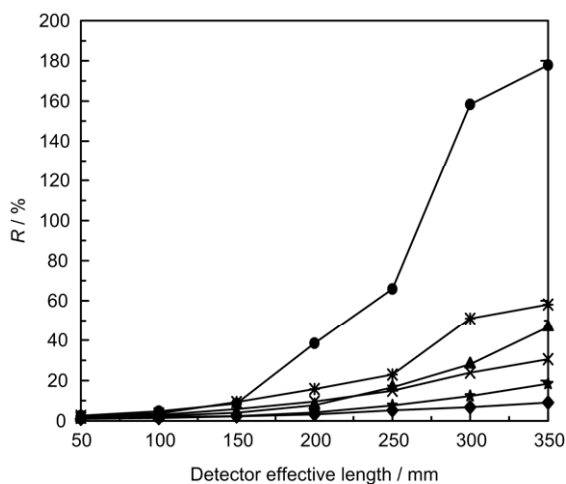


Fig.5 Near-to-far detector response ratio vs. detector effective length at different porosities of the water- and oil-sandstone. Porosities: ◆10%, ★20%, ▲30%, ×40%, ※50%, ●60%

3.5 Simulation of water- or oil-sandstone

The simulation conditions were the same in Section 3.4, with either water-sandstone or oil-sandstone, in porosity of 10%, 20%, 30%, 40%, 50% and 60% (Fig. 6). The R increases with the porosity for both

sandstones, but R with oil sandstone is a bit greater than with water sandstone.

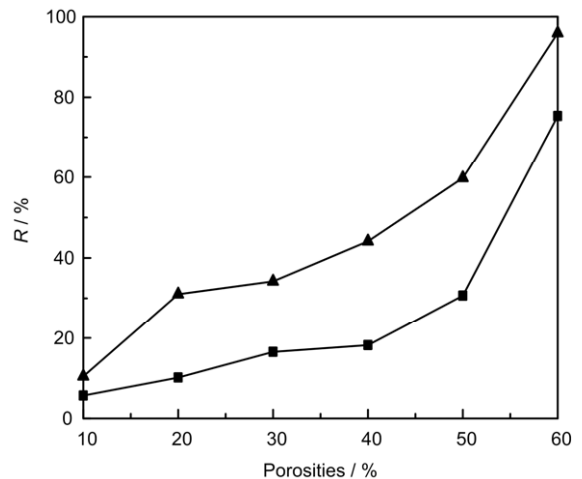


Fig.6 Near-to-far detector response ratio at different porosities of water- and oil-sandstone.

■water-sandstone, ▲oil-sandstone

4 Conclusion

The near-to-far detector response ratio increases with the porosity of sandstone. According to the simulation, the optimum conditions for CNL are 80 mm thick lead plus 1 cm thick LiOH shield in front of the near detector, and the near-to-far detector distance of 250 mm.

References

- 1 Ding D Z, Ye C T, Zhao Z X. Neutron physics: principles, methods and applications. Beijing: Atomic Energy Press, 2001, 951–961 (in Chinese).
- 2 Tuo X G, Mu K L, Lei J R, *et al.* Nucl Tech, 2007, **30**: 388–390 (in Chinese).
- 3 Hearsta J R. Nucl Instrum Methods, 1974, **117**: 141–151.
- 4 Serov I V, John T M, Hoogenboom J E. Appl Radiat Isot, 1998, **49**: 1737–1744.
- 5 Zhang J M, Xia L Z, Qiu Y X, *et al.* At Energy Sci Technol, 2006, **40**: 125–128 (in Chinese).
- 6 Xia L Z, Zhang J M, Yang Z G, *et al.* Well Logging Technol, 2003, **27**: 477–480 (in Chinese).
- 7 Pang J F. Nuclear logging physics basis. Beijing: Petroleum Industry Press, 2005, 127–128 (in Chinese).
- 8 Qiu Y X, Xia L Z, Peng H, *et al.* Well Logging Technol, 2004, **28**: 471–477 (in Chinese).
- 9 Briesmeister J F. MCNPTM-A general monte carlo N-Particle transport Code (4C), Los Alamos, New Mexico: Los Alamos National Laboratory, 2000.

Partially supported by National Key Technology R&D Program of China(2008BAK47B04), Innovation Method Work(2008IM040500), National Natural Science Foundation of China(40673058) and Sichuan province Key Technology R&D Program(2008GZ0040, 2008GZ0197)

* Corresponding author. *E-mail address*: bjyang9@163.com

Received date: 2009-04-27